

Compliant Ankles and Flat Feet for Improved Self-Stabilization and Passive Dynamics of the Biped Robot “RunBot”

Poramate Manoonpong, Tomas Kulvicius,
and Florentin Wörgötter

Bernstein Center for Computational Neuroscience,
The Third Institute of Physics, University of Göttingen
37077 Göttingen, Germany

Email: (poramate, tomas, worgott)@physik3.gwdg.de

Lutz Kunze, Daniel Renjewski,
and Andre Seyfarth

Lauflabor Locomotion Laboratory,
University of Jena,
07743 Jena, Germany

Email: L.Kunze22@web.de, (daniel.renjewski, oas)@uni-jena.de

Abstract—Biomechanical studies of human walking reveal that compliance plays an important role at least in natural and smooth motions as well as for self-stabilization. Inspired by this, we present here the development of a new lower leg segment of the dynamic biped robot “RunBot”. This new lower leg segment features a compliant ankle connected to a flat foot. It is mainly employed to realize robust self-stabilization in a passive manner. In general, such self-stabilization is achieved through mechanical feedback due to elasticity. Using real-time walking experiments, this study shows that the new lower leg segment improves dynamic walking behavior of the robot in two main respects compared to an old lower leg segment consisting of rigid ankle and curved foot: 1) it provides better self-stabilization after stumbling and 2) it increases passive dynamics during some stages of the gait cycle of the robot; i.e., when the whole robot moves unactuated. As a consequence, a combination of compliance (i.e., the new lower leg segment) and active components (i.e., actuated hip and knee joints) driven by a neural mechanism (i.e., reflexive neural control) enables RunBot to perform robust self-stabilization and at the same time natural, smooth, and energy-efficient walking behavior without high control effort.

I. INTRODUCTION

Humans walk with a dynamic, robust, and energy-efficient gait. They can adapt quickly to terrain changes and even learn to walk differently on different surfaces. Neurophysiological studies have revealed that these abilities are achieved through the interactions between neural control [1] and biomechanics [2]. For instance, we can perform a variety of walking behaviors with simultaneous self-stabilization against unexpected disturbances (stumbling over obstacles) because of our appropriate biomechanical structure. At the same time, neural control plays a role in locomotion generation and assures that different gaits can first be learned and then quickly applied to adapt to the terrain.

During the last few decades roboticists have intensively employed neurophysiological findings to develop biped robots showing human walking characteristics, e.g., adaptivity, dynamics, energy efficiency, and self-stabilization. Recent studies have emphasized the importance of structure design by concentrating on so-called passive dynamic walkers, which

are simple devices that can walk stably down a slope [3], [4]. This is achieved only by their biomechanics. Adding actuators to their joints may allow these robots to walk also on a level surface or even uphill. The developed gaits are impressively human-like [5]. Other advanced ZMP-based biped walkers, like ASIMO [6], HRP [7], LOLA [8], WABIAN [9], HUBO [10], have been built consisting of several active joints, for instance, hip, knee, ankle and trunk joints but their designs have paid less attention to passive dynamic walking. Thus, they require a lot of energy, which is in conflict with measured human power consumption during walking [11]. Although all these walkers are impressive in their own right, their constructions are generally based on engineering design using rigid components instead of compliant joints which play an important role in human walking. Employing such elastic components can reduce the control effort for stable locomotion [12]. They provide mechanical feedback called reflexes [2], [13] to the systems leading to robust self-stabilization. In other words, reflexes are passive mechanisms that rapidly stabilize motion in response to unexpected perturbations. Following this concept, there are approaches that employ *passive* compliant joints on biped robots as well as animal-like robots to achieve locomotion and obtain passive self-stabilization. Most of them have reported results from simulations [11], [14], [15], [16], [17] while a few have used real biped robots [12], [18], [19] and real animal-like robots [20], [21], [22], [23].

To tackle the challenge towards human-like walking in biped robots, we continue in this tradition emphasizing the coupling of biomechanics and neural control. We have developed the RunBot series of dynamic planar biped robots, in a stepwise manner during the last years [24], [25], [26], [27]. RunBot has achieved a relative walking speed of 3.5 leg-lengths per second, which is comparable to the maximal relative speed of human walking. It is under real-time neural control by ways of a small network allowing it to walk at different walking speeds and to learn to adapt its locomotion to different terrains, e.g., level floor versus up a ramp. Although RunBot has shown a certain degree of human-like

gait characteristics and adaptivity under neural control, it still lacks compliant mechanisms. Thus, a goal of this study is to improve the mechanical design focusing on replacing its rigid curved feet with a compliant ankle connected to a flat foot. This design is inspired by a biomechanical study of human walking suggesting that ankle joints show compliant behavior during part of the stance and during the entire swing phase [11]. This introduces flexibility to the joints and makes foot landing soft, leading to natural and smooth locomotion as well as robust self-stabilization, e.g., after having stumbled.

The paper is organized as follows. First we describe a mechanical setup of the latest version of the RunBot series, and the new design of its lower leg segment. Second, we present the reflexive neural control for locomotion generation. Third, we illustrate the performance of the new lower leg segment focusing on compliance, self-stabilization, and passivity. Finally, we provide conclusions and discuss future work.

II. BIPED ROBOT WITH COMPLIANT ANKLES AND FLAT FEET

A. The biped robot RunBot

RunBot is a planar biped walking robot, 26 cm tall from foot to hip joint axis (see Fig. 1(a)). It has a total weight of about 600 g. It is held sagittally by a boom of about 80 cm length, so that it cannot fall sideways, while a freely rotating joint of the boom influences the walking dynamics in no way other than that RunBot is constrained on a circular path. Its legs have four actuated joints: left hip (LH), right hip (RH), left knee (LK) and right knee (RK). Each joint is driven by an RC (radio controlled) servo motor where the built-in pulse width modulation (PWM) control circuit is disconnected while its built-in potentiometer is used to measure the joint angles. A mechanical stopper is implemented on each knee joint to prevent it from going into hyperextension, similar to the function of human kneecaps. Approximately seventy percent of the robot's weight is concentrated on its trunk, and the parts of the trunk are assembled in a way that its center of mass is located forward of the hip axis. RunBot's design also relies on the principles of passive walking characteristics reflected by the fact that during some stages of every step cycle all motor voltages remain zero.

RunBot has now a new lower leg segment consisting of a flat foot and a compliant ankle with extension and torsion springs (see Fig. 1c). The leg segment is equipped with a switch sensor to detect ground contact events. These new features allow the robot to perform better self-stabilization and achieve more passivity (see Sect. IV) compared to the old one (see Fig. 1b). Hip and knee joints are driven by output signals of a reflexive neural controller (running on a PC) through the Meilhaus card ME-2600 board with an update frequency of 250 Hz. The signals of the joint angles and ground contact switches are also digitized by this board for the purpose of feeding them into the neural controller. Further details of the robot can be found in [26].

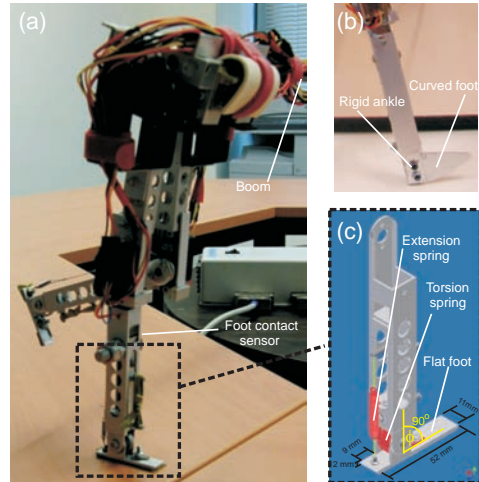


Fig. 1. Biomechanical components of the biped robot RunBot. (a) RunBot with new lower leg segment developed in collaboration between the Locomotion Laboratory in Jena and the Bernstein Center for Computational Neuroscience, Göttingen. (b) Old lower leg segment consisting of curved foot and rigid ankle based on passive walkers [5]. (c) 3D model of the new lower leg segment consisting of flat foot and compliant ankle with extension and torsion springs inspired by a biomechanical study of human walking [11].

B. Design of the new lower leg segment with compliant ankle and flat foot

Experimental research of human walking reveals that ankle joints exhibit compliance (spring like behavior) [11]. This evidence forms the basis of the development of the new lower leg segment with compliant ankle and flat foot. In addition, there are also other reasons pushing us to the new design which can be summarized as follows: first, curved feet with rigid ankle of the old lower leg segment (see Fig. 1b) do not look human-like. Second, the old lower leg segment confines RunBot's behavior only to walking but not to, e.g., standing still in an upright position on one leg (see Fig. 1a). Third, compliant ankles and flat feet seem to have a positive effect on the disturbance compensation behavior of the robot, i.e., leading to robust self-stabilization, as compared to the old design. Finally, in real world applications, like foot-prostheses, compliant springs can support a compression of ground and improve roll-off behavior [28].

Here, we develop the new lower leg segment in a way that its compliance (spring mechanisms) works in the ankle axis. We use the method of Morasso and Schieppati [29] to approximate the minimum value of ankle stiffness, according to:

$$c_a = mgl. \quad (1)$$

The resulting ankle stiffness c_a is ≈ 1530 Nmm/rad (or ≈ 26 Nmm/ $^\circ$) with $m = 600$ g (mass of RunBot), $g = 9.81$ m/s 2 (earth's gravity) and $l = 26$ cm (leg length, see Fig. 2). This stiffness c_a ensures standing in upright position on both legs. Thus, the total spring stiffness of one ankle can be estimated in the range of $c_a/2, \dots, c_a$. As described in [11], ankle torques

without spring T_a and with linear spring T_s can be calculated, according to:

$$T_a = F_g l \cos \phi \quad (2)$$

$$T_s = c_t \Delta \phi \quad (3)$$

where F_g is RunBot's weight, l is the leg length, and ϕ is the rotation angle of the ankle joint (see Fig. 2). c_t is the linear spring stiffness, i.e., here $c_a/2, \dots, c_a$, and $\Delta \phi$ is the angle difference between the resting and actual angle of the ankle joint. Note that, RunBot has a resting angle of 90° (see Figs. 1c and 2).

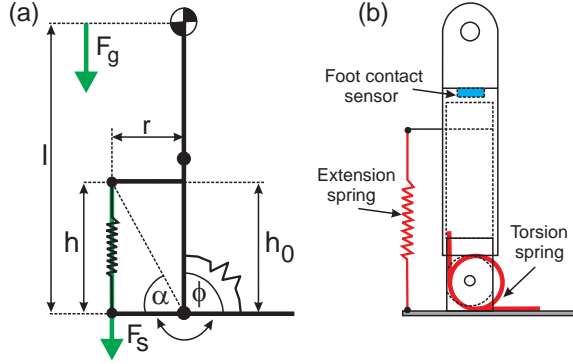


Fig. 2. (a) Leg geometry consisting of upper and lower leg segments with spring mechanisms (see text for parameter details). (b) Layout of the lower leg segment.

Figure 3a shows a curve of the nonlinear ankle torque of RunBot without spring (calculated from Eq. 2) and the curves of the linear ankle torque with the spring at different stiffness (calculated from Eq. 3). According to the torque-angle curves, for simplification we could use one torsion spring in each ankle where its stiffness should be slightly below the nonlinear ankle torque curve since above the curve the springs are too stiff and compliance is lost. However, there are no torsion springs which can be fitted into the new lower leg segment with respect to the required stiffness and a specific size of 18 mm maximum diameter and 8 mm maximum width. The closest one is the T-18917L torsion spring¹ having a spring stiffness of 10.65 Nmm/ $^\circ$ which is too soft to obtain stable walking. For this reason an extension spring is implemented as achilles tendon linking between the heel and the lower leg segment (see Figs. 1 and 2) in order to obtain the desired compliant behavior (i.e., appropriate spring stiffness) and stable walking. The spring force F_s is estimated over a change of the angle ϕ of the ankle joint, according to:

$$F_s = c_e(h - h_0) \quad (4)$$

$$h = \sqrt{2r^2 + h_0^2 - 2r\sqrt{r^2 + h_0^2} \cos \alpha} \quad (5)$$

¹It has a size of 17.1 mm outer diameter and 7.65 mm width and is made of stainless steel EN 10270-3-1.4310, <http://www.federnshop.com>.

$$\alpha = 180^\circ - \arctan\left(\frac{r}{h_0}\right) - \phi \quad (6)$$

where c_e is the linear spring stiffness, e.g., 0, ..., 7 N/mm, h is the spring length, which changes according to ϕ , h_0 is the resting length of the spring system, i.e., here 52.5 mm, r is the distance between the spring and the ankle joint, i.e., here 11.5 mm, α and ϕ are angles with respect to leg configuration (see Fig. 2a). Figure 3b shows the force-angle curves of the spring with different stiffness in a range of 0, ..., 7 Nmm/ $^\circ$. To find an appropriate one, we also tested the different springs with respect to the estimated forces (see Fig. 3b) on the real robot. As a result, we use the Z075E-01X extension spring² having a stiffness of 4.745 N/mm and a size of 7.8 mm outer diameter and a length of 18.7 mm. The advantage of introducing this extension spring is that we could easily increase or decrease compliance of the system by exchanging this spring instead of the torsion spring which is more difficult. For the foot, we design it in proportion to the leg length of RunBot compared to the human foot-to-leg ratio. As a result, it has a size of 11 x 52 x 2 mm (see Fig. 1c).

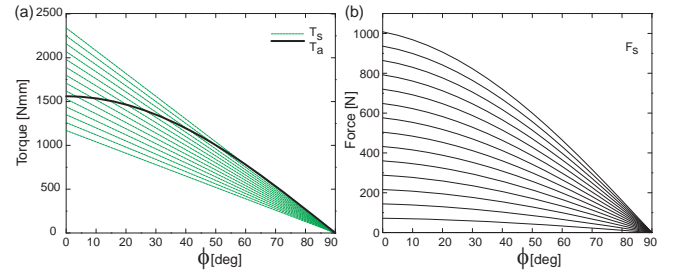


Fig. 3. (a) Torque-angle curve of RunBot without spring (T_a , black) and torque-angle curves of a linear torsion spring with varying stiffness in a range of $c_t = 13, \dots, 26$ Nmm/ $^\circ$ (T_s , green). (b) Force-angle curves of a linear extension spring with varying stiffness in a range of $c_e = 0, \dots, 7$ Nmm/ $^\circ$.

III. REFLEXIVE NEURAL CONTROLLER

We use a reflexive neural controller (see Fig. 4) to generate locomotion of the robot. The controller is based on a hierarchical design and simulated as mono-synaptic connections containing flexor N_F and extensor N_E motor neurons for each hip and knee. The motor neurons are linear and can send their signals unaltered to the motors M . Furthermore, there are several local nonspiking sensory neurons (rate coded neurons), which by their conjoint reflex-like actions trigger the different walking patterns. These local sensor neurons can be classified into three local loops: joint control ($Local_1$), intra-joint control ($Local_2$) and leg control ($Local_3$). Joint control arises from sensors S at each joint, which measure the joint angle and influence only their corresponding motor neurons. Intra-joint control is achieved from sensors A , which measure the anterior extreme angle (AEA) at the hip and trigger an extensor reflex at the corresponding knee. Leg control comes from ground contact sensors G , which influence the motor

²It is made of stainless steel EN 10270-1-DH, <http://www.federnshop.com>.

neurons of all joints. In general, the reflexive locomotion generation works as follows: When one foot touches ground the hip extensor and knee flexor of the other leg (swing leg) are triggered, as well as the hip flexor and knee extensor of the stance leg. When the hip stretch receptor of the swing leg is activated, the extensor of the knee joint in this leg is triggered. Finally the foot of the swing leg touches the ground and the swing leg and the stance leg swap their roles thereafter. Further details of the controller are not subject of this study, but can be found in [27]. It is important to note that in this study we fix synaptic weights of the controller such that it will only generate basic locomotion while gait stabilization will be mainly achieved through biomechanics; i.e., a non-neural feedback loop (preflexes [2], [21], [30]). In other words, RunBot can perform dynamic walking with passive self-stabilization to disturbances (i.e., stumbling over obstacles, see Sect. IV) without changing the controller parameters gaining for more robustness than in previous studies [24], [25], [27].

In contrast to other walking robot controllers, our neural controller has no central pattern generator in the form of a neural oscillator. Rhythmic patterns are generated by the whole system using the electrical and mechanical properties of the motors, the limbs, and the feedback from the environment. In addition, it does not employ any kind of position or trajectory-tracking control algorithm [6], [7], [8], [9], [10]. Instead, it allows our biped robot to exploit its own natural dynamics during critical stages of its walking gait cycle.

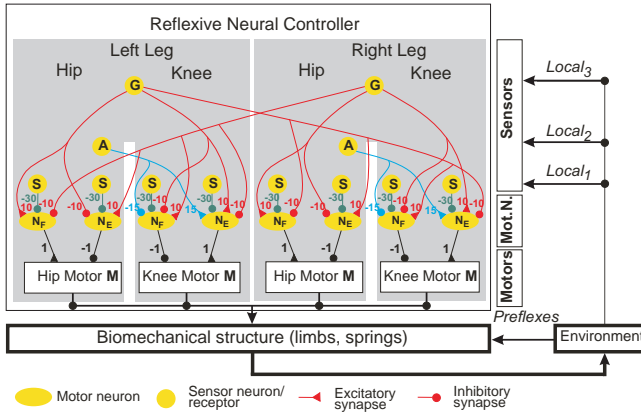


Fig. 4. Reflexive neural network. The connection strengths (colored lines) are indicated by the small numbers. G refers to the ground contact sensor neurons of the feet and A to the stretch receptors for AEA of the hips. S represents the angle sensor neurons of each joint. $N_F(N_E)$ refers to flexor (extensor) motor neuron of the leg. The black box at the bottom represents RunBot’s physical embodiment. Walking control basically arises from the interplay of the different sensorimotor loops ($Local_{1,2,3}$) implemented in RunBot together with its passive dynamic walking and self-stabilization properties (preflexes).

IV. ROBOT WALKING EXPERIMENTS

Three main experiments were carried out to assess the performance of the new lower leg segment consisting of compliant ankle and flat foot. Experiments present (1) the basic function of the compliant ankles in analogy to human ankles, (2) robust self-stabilization to disturbances, and (3)

passive walking capability. In all experiments we let RunBot walk at a speed of ≈ 40 cm/s on flat terrain with an obstacle that cannot be detected during walking. We use stacks of rubber sheets as the obstacle where each sheet has a size of $5.5 \times 5.5 \times 0.3$ cm.

In the first experiment, we demonstrate the basic function of the compliant ankles. Here, we use four sheets as obstacle having a total height of 1.2 cm ($\approx 5\%$ of robot size). This is the maximum height that RunBot can tackle without changing its control parameters. With this height one can also clearly observe elasticity of the ankles, e.g., extension of the ankle when the foot hits the obstacle. Figure 5 shows that the ankle can passively extend similar to a human ankle. Due to compliance, RunBot can simply free its foot after hitting the obstacle and continue to walk. In addition to this, the passive extension and flexion of the ankles allow RunBot to walk naturally with stable and smooth motions. We strongly encourage readers to watch a video clip of the experiment (Supplementary Video) at <http://www.manoonpong.com/Humanoid2011/SupplVideo.wmv>.

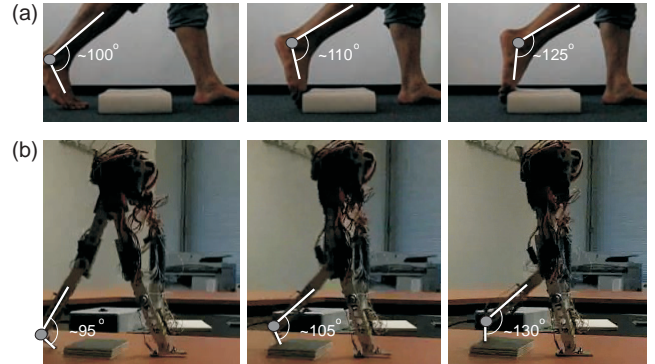


Fig. 5. Snap shots produced by a high-speed camera illustrate ankle extension of human and RunBot while their foot hits an obstacle. (a) Human’s ankle extension. (b) RunBot’s ankle extension.

In the second experiments, we show the robust passive self-stabilization property of the new lower leg segment when RunBot stumbles over an obstacle. In addition, we also compare its performance to the curved foot with rigid ankle. In both cases we use the same neural controller for generating locomotion on a flat terrain. Here, we use three sheets having a total height of 0.9 cm as obstacle since RunBot cannot deal with higher obstacles than this with its old lower leg segment. Figure 6 shows three different cases of RunBot’s foot approaching the obstacle and a comparison of using the new and old lower leg segments. RunBot with the new lower leg segment can successfully perform self-stabilization when it stumbles while with the old one it fails most of the time (see Supplementary Video at <http://www.manoonpong.com/Humanoid2011/SupplVideo.wmv>).

Figure 7 exemplifies hip and knee angle sensor signals of a perturbed walking gait where RunBot uses the new lower leg segment. Deviations of the signals are caused by external disturbances such as hitting an obstacle during swing phase

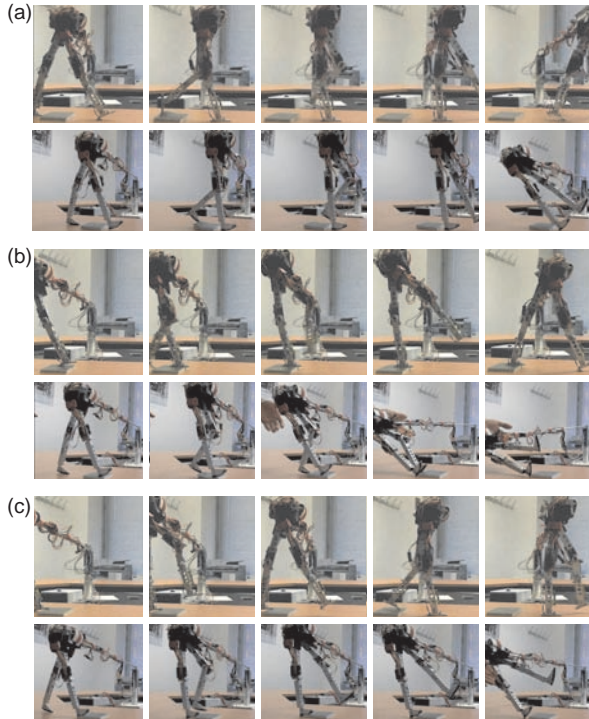


Fig. 6. Snap shots produced by a high-speed camera show a comparison of walking behavior using new (top) and old (bottom) lower leg segments when the foot approaches an obstacle at different foot locations. (a) *Case I*: Leading foot of RunBot steps over the obstacle while following foot hits it. Using its new lower leg segment (top), RunBot can stably stand on its leading foot since it is flat and then it can swing its following foot across the obstacle without getting stuck. In contrast, using its old lower leg segment (bottom), RunBot cannot stably stand while it swings its following foot. In addition, its following foot gets stuck shortly during swing phase. As a consequence, RunBot falls back. (b) *Case II*: Leading foot of RunBot steps on the obstacle while following foot hits it. Using its new lower leg segment (top) shows almost a similar effect as described in *Case I* but using its old one (bottom) results in getting stuck heavily by the following foot such that RunBot falls back. (c) *Case III*: Leading foot of RunBot steps on the edge of the obstacle while following foot swings across it without hitting. In this case, the spring mechanism of its new lower leg segment of the stance leg keeps RunBot balanced by providing an additional force pushing it forward. As a consequence, RunBot can keep on walking without trouble (top). In contrast, its old lower leg segment of the stance leg has no such force to push it forward such that it falls back (bottom).

(compare, e.g., *Case I*, Fig. 6a (top)). After the disturbances, the signal trajectories soon return to normal periodic patterns, demonstrating that the walking gait is stable and to some degree robust against external disturbances. Here, robustness is defined as rapid convergence to a steady-state behavior in spite of unexpected perturbations. That is, RunBot does not fall and continues walking. By contrast, using the old lower leg segment, the hip and knee angle sensor signals do not return to normal periodic patterns after perturbations (not shown). They stay at specific angle values and RunBot falls.

In addition to the above experiments, we also tested RunBot in four different experiments to compare its walking performance using new and old legs on flat terrain with an obstacle. Experiment I uses one rubber sheet (0.3 cm height) as obstacle, Experiment II two rubber sheets (0.6 cm height), Experiment

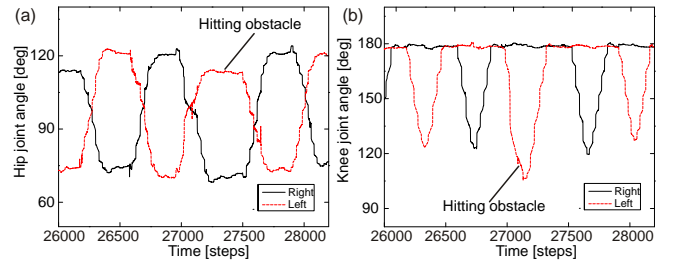


Fig. 7. Perturbed walking signals. (a) Hip angle sensor signal of *Case I* (Fig. 6a, top). (b) Knee angle sensor signal of *Case I* (Fig. 6a, top). It can be seen that after being perturbed the walking gait returns to its normal pattern quickly in only one step. The signals of other cases using the new lower leg segment show also slightly similar patterns; i.e., returning to their normal periodic patterns quickly after perturbations (not shown). Here, RunBot can neither detect the perturbations nor adjust any parameters of its controller to compensate for them. Thus, its stabilization mainly is derived from its biomechanics (preflexes, see lowest loop in Fig. 4).

III three rubber sheets (0.9 cm height), and Experiment IV four rubber sheets (1.2 cm height). Figure 8a shows a comparison of the success rate³ of the new and old lower leg segments. It can be seen that both show similar results in Experiments I and II; i.e., RunBot can deal with obstacles having a height of 0.3 and 0.6 cm without falling (100 % success rate). On the other hand, Experiments III and IV show that RunBot using its old lower leg segment has very low success rates compared to the new one. This shows that the new lower leg segment allows RunBot to better perform self-stabilization against a higher degree of disturbances.

In the last experiments, we observe and present the passive walking capability of RunBot using the new lower leg segment. We let RunBot walk on flat terrain without obstacles. Figure 8b presents the passive properties of RunBot due to the biomechanical design. Although the motor voltages are zero, the interplay of the appropriate weight, the generated velocity, the compliance of the ankles, and the flat feet leads to a momentum, which is high enough to rotate the joint and swing the leg into the desired position. At the same time the gear friction will decrease the acceleration. It can be seen that RunBot with its new lower leg segment can perform passive walking during about 32 % of one gait cycle which is larger than with its old one which remains passive for only about 25 % (not shown but see [27]).

V. CONCLUSION AND FUTURE WORK

We developed a new lower leg segment of RunBot consisting of flat foot and compliant ankle with extension and torsion springs. The design of this leg segment partly mimics the function of the human's lower leg segment. Using real-time walking experiments, this study has shown that the new lower leg segment provides better mechanical feedback (known as reflexes [2], [21], [30]) to the system than the old one with rigid curved foot. As a consequence, combination of compliance (i.e., the new lower leg segment) and active

³Percentage of success in total number of experiments. Here, each experiment is repeated ten times.

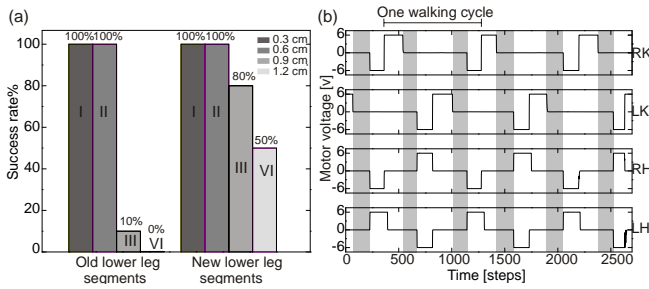


Fig. 8. (a) Comparison of the success rates of the new and old lower leg segments. Histogram showing the average of success rate of each experiment. We place obstacles with different heights on flat terrain: Experiment I: 0.3 cm. Experiment II: 0.6 cm. Experiment III: 0.9 cm. Experiment IV: 1.2 cm. Each experiment of each leg type is repeated ten times. (b) Passive walking with the new lower leg segment. Motor voltages directly sent from the leg motor neurons through motor amplifiers while RunBot is walking: LH, left hip; RH, right hip; LK, left knee; RK, right knee. Gray areas indicate when all four motor voltages remain zero during part of every step cycle; i.e., RunBot walks passively.

components (i.e., actuated hip and knee joints) driven by a neural mechanism (i.e., reflexive neural control) enables RunBot to perform robust self-stabilization and at the same time natural, smooth, and energy-efficient walking behavior without high control effort. We believe that this is one of the promising approaches towards advanced dynamic walking robots which are capable of exploiting their own biomechanics for locomotion in a passive manner and use neural mechanisms for active locomotion and adaptation [27].

More demanding tasks will be the use of deviation information of proprioceptive sensor signals (hip and knee joint angles, Fig. 7) together with additional exteroceptive sensors, e.g., infrared eyes, and neural learning [27] to allow RunBot to anticipate obstacles and change its gait before approaching them. This way, it could tackle higher obstacles and perform more stable locomotion in an adaptive manner.

ACKNOWLEDGMENTS

This research was supported by the Deutsche Forschungsgemeinschaft (DFG, SE1042/05), the Emmy Noether Program of the Deutsche Forschungsgemeinschaft (DFG, MA4464/3-1), and the Federal Ministry of Education and Research (BMBF) by a grant to the Bernstein Center for Computational Neuroscience II Göttingen (01GQ1005A, project D1).

REFERENCES

- [1] G. N. Orlovsky, T. G. Deliagina, and S. Grillner, *Neuronal control of locomotion: From mollusk to man*. Oxford University Press, 1999.
- [2] M. H. Dickinson, C. T. Farley, R. J. Full, M. A. R. Koehl, R. Kram, and S. Lehman, "How animals move: An integrative view," *Science*, vol. 288, pp. 100–106, 2000.
- [3] S. Collins, M. Wisse, and A. Ruina, "A 3-d passive dynamic walking robot with two legs and knees," *Int. J. Robot. Res.*, vol. 20, pp. 607–615, 2001.
- [4] T. McGeer, "Passive dynamic walking," *Int. J. Robot. Res.*, pp. 62–82, 1990.
- [5] S. Collins, A. Ruina, R. Tedrake, and M. Wisse, "Efficient bipedal robots based on passive dynamic walkers," *Science*, vol. 307, pp. 1082–1085, 2005.
- [6] M. Hirose and K. Ogawa, "Honda humanoid robots development," *Phil. Trans. R. Soc. A*, vol. 365, pp. 11–19, 2007.

- [7] H. Hirukawa, F. Kanehiro, K. Kaneko, S. Kajita, K. Fujiwara, and et al., "Humanoid robotics platforms developed in HRP," *Robotics and Autonomous Systems*, vol. 48, pp. 165–175, 2004.
- [8] H. Ulbrich, T. Buschmann, and S. Lohmeier, "Development of the humanoid robot LOLA," *Applied Mechanics and Materials*, vol. 5–6, pp. 529–539, 2006.
- [9] Y. Ogura, H. Aikawa, K. Shimomura, A. Morishima, H. ok Lim, and A. Takanishi, "Development of a new humanoid robot wabian-2," in *IEEE International Conference on Robotics and Automation*, 2006, pp. 76–81.
- [10] J.-Y. Kim, I.-W. Park, J. Lee, M.-S. Kim, B. kyu Cho, and J.-H. Oh, "System design and dynamic walking of humanoid robot KHR-2," in *IEEE International Conference on Robotics and Automation*, 2005, pp. 1431–1436.
- [11] S. W. Lipfert, *Kinematic and Dynamic Similarities between Walking and Running*. Verlag Dr. Kovac, 2010.
- [12] F. Iida, Y. Minekawa, J. Rummel, and A. Seyfarth, "Toward a human-like biped robot with compliant legs," *Robotics and Autonomous Systems*, pp. 139–144, 2009.
- [13] J. C. Spagna, D. I. Goldman, P.-C. Lin, D. E. Koditschek, and R. J. Full, "Distributed mechanical feedback in arthropods and robots simplifies control of rapid running on challenging terrain," *Bioinsp. Biomim.*, vol. 2, pp. 9–18, 2007.
- [14] K. D. Farrell, C. Chevallereau, and E. R. Westervelt, "Energetic effects of adding springs at the passive ankles of a walking biped robot," in *IEEE International Conference on Robotics and Automation*, 2007, pp. 3591–3596.
- [15] H. Geyer, A. Seyfarth, and R. Blickhan, "Compliant leg behaviour explains basic dynamics of walking and running," *Proc. R. Soc. B*, vol. 273, pp. 2861–2867, 2006.
- [16] T. Schauss, M. Scheint, M. Sobotka, W. Seiberl, and M. Buss, "Effects of compliant ankles on bipedal locomotion," in *IEEE International Conference on Robotics and Automation*, 2009, pp. 2761–2766.
- [17] K. Y. Yi, "Walking of a biped robot with compliant ankle joints," in *IEEE/RSJ International Conference on Intelligent Robots and Systems*, vol. 1, 1997, pp. 245–250.
- [18] A. Seyfarth, F. Iida, R. Tausch, M. Stelzer, O. von Stryk, and A. Karguth, "Towards bipedal jogging as a natural result for optimizing walking speed for passively compliant three-segmented legs," *Int. J. Robot. Res.*, vol. 28, pp. 257–265, 2009.
- [19] M. Wisse, D. G. E. Hobbelen, R. J. J. Rotteveel, S. O. Anderson, and G. J. Zeglin, "Ankle springs instead of arc-shaped feet for passive dynamic walkers," in *IEEE International conference on Humanoid Robots*, 2006.
- [20] Y. Fukuoka, H. Kimura, and A. H. Cohen, "Adaptive dynamic walking of a quadruped robot on irregular terrain based on biological concepts," *Int. J. Robot. Res.*, vol. 22, pp. 187–202, 2003.
- [21] J. G. Cham, J. K. Karpick, and M. R. Cutkosky, "Stride period adaptation of a biomimetic running hexapod," *Int. J. Robot. Res.*, vol. 23, pp. 141–153, 2004.
- [22] N. Neville and M. Buehler, "Towards bipedal running of a six legged robot," in *12th Yale Workshop on Adaptive and Learning Systems*, 2003.
- [23] P. Manoonpong, F. Wörgötter, and F. Pasemann, "Biological inspiration for mechanical design and control of autonomous walking robots: Towards life-like robots," *The International Journal of Applied Biomedical Engineering (IJABME)*, vol. 3, pp. 1–12, 2010.
- [24] T. Geng, B. Porr, and F. Wörgötter, "A reflexive neural network for dynamic biped walking control," *Neural Comput.*, vol. 18, pp. 1156–1196, 2006.
- [25] T. Geng, B. Porr, and F. Wörgötter, "Fast biped walking with a sensor-driven neuronal controller and real-time online learning," *Int. J. Robot. Res.*, vol. 25, pp. 243–259, 2006.
- [26] L. Kunze, "Elektromechanische modellierung und leistungsvergleich am zweibeinigen roboter runbot mit elastischem fussgelenk," Master's thesis, University of Jena, 2010.
- [27] P. Manoonpong, T. Geng, T. Kulvicius, B. Porr, and F. Wörgötter, "Adaptive, fast walking in a biped robot under neuronal control and learning," *PLoS Comput. Biol.*, vol. 3, no. 7, p. e134, 2007.
- [28] S. Blumentritt, H. W. Scherer, and U. Wellershaus, "Biomechanisch-ganganalytische bewertung von prothesenfuessen," *Medizinisch-Orthopaedische Technik*, pp. 287–292, 1994.
- [29] P. G. Morasso and M. Schieppati, "Can muscle stiffness alone stabilize upright standing?," *J. Neurophysiol.*, vol. 83, pp. 1622–1626, 1999.
- [30] R. Full and D. Koditschek, "Templates and anchors: neuromechanical hypotheses of legged locomotion on land," *Journal of Experimental Biology*, vol. 202, pp. 3325–3332, 1999.